minerals

MDPI

Article

U-Th-He Geochronology of Pyrite from the Uzelga VMS Deposit (South Urals)—New Perspectives for Direct Dating of the Ore-Forming Processes

Olga Yakubovich [1,2,*], Mary Podolskaya [3], Ilya Vikentyev [4,5], Elena Fokina [1] and Alexander Kotov [2]

1 Institute of Earth Sciences, Saint-Petersburg University, Universitetskaya emb., 7/9, 199034 Saint-Petersburg, Russia; albite@yandex.ru
2 Institute of Precambrian Geology and Geochronology (IPGG) Russian Academy of Sciences, Makarova emb. 2, 199034 Saint-Petersburg, Russia; abkotov-spb@mail.ru
3 Vernadsky institute of geochemistry and analytical chemistry (GEOKHI) Russian Academy of Sciences, Kosygina str. 19, 119991 Moscow, Russia; marypodolskaya@gmail.com
4 Institute of Geology of Ore Deposits, Petrography, Mineralogy and Geochemistry (IGEM), Russian Academy of Sciences, Staromonetny per. 35, 119017 Moscow, Russia; viken@igem.ru
5 Engineering Academy, Peoples' Friendship University of Russia (RUDN University), Miklukho-Maklaya str. 6, 117198 Moscow, Russia
* Correspondence: olya.v.yakubovich@gmail.com

Received: 27 April 2020; Accepted: 11 July 2020; Published: 16 July 2020

Abstract: We report on the application of the U-Th-He method for the direct dating of pyrite and provide an original methodological approach for measurement of U, Th and He in single grains without loss of parent nuclides during thermal extraction of He. The U-Th-He age of ten samples of high-crystalline stoichiometric pyrite from unoxidized massive ores of the Uzelga volcanogenic massive sulfide (VMS) deposit, South Urals, is 382 ± 12 Ma (2σ) (U concentrations ~1–5 ppm; ^{4}He ~10^{-4} cm^3 STP g^{-1}). This age is consistent with independent (biostratigraphic) estimations of the age of ore formation (ca, 389–380 Ma) and is remarkably older than the probable age of the regional prehnite-pumpellyite facies metamorphism (~340–345 Ma). Our results indicate that the U-Th-He dating of ~1 mg weight pyrite sample is possible and open new perspectives for the dating of ore deposits. The relative simplicity of U-Th-He dating in comparison with other geochronological methods makes this approach interesting for further application.

Keywords: geochronology; helium dating; pyrite; Uzelga; VMS deposits

1. Introduction

Isotope systems based on radiogenic helium are traditionally used in the field of low-temperature thermochronology mainly for evaluation of rock exhumation rates at shallow crustal levels [1], for dating volcanic eruptions [2] and regional weathering events [3]. Although, He can easily migrate from the crystal structures of most minerals over geological history [1], its preservation in native metals is very high [4]. Recent developments in understanding the behavior of He in minerals allowed Yu.A. Shukolyukov with co-authors to propose a new ^{190}Pt-^{4}He method of isotope geochronology [5]. The method was successfully applied for dating Pt-Fe alloys from various deposits worldwide [6,7]. In addition, it was shown to be promising for dating sperrylite ($PtAs_2$) [8]. The ^{190}Pt-^{4}He ages of this mineral from Norilsk (242 ± 12 Ma) and Kondyor (122 ± 6 Ma) deposits are consistent with biotite Ar-Ar ages, ~245–250 and 120 ± 1 Ma, respectively [9,10]. High retention of He in sperrylite suggests that pyrite, which has the same crystallographic structure, might also be a convenient mineral for

geochronology. Recent experiments on helium thermodesorption from sulfides had confirmed this suggestion [11] and preliminary results of the U-Th-He dating of pyrite from the Uzelga deposit are promising [12].

Pyrite is abundant in the most of the ore deposits [13–16]) and is a common accessory mineral of igneous and sedimentary rocks [13,17]. Therefore, pyrite geochronology has a range of potential applications. In particular, the timing of ore-forming processes is a critical component in the development of genetic models for ore formation. In fact, tectonics, magmatism, and/or sedimentary basin evolution may exert a large-scale control on ore formation but this can be difficult to prove without robust age constraints [18].

Traditionally, sulfide mineralization is directly dated by the Re-Os method. Re-Os geochronology of molybdenite, pyrite and arsenopyrite has widely and successfully been used to date a large variety of ore types including orogenic gold, porphyry, sedimentary exhalative and Mississippi Valley-type deposits [19–24]. However, the results produced by pyrite Re-Os geochronology are complex and show a high degree of scatter and/or imprecise ages [23,25,26]. At present, it is clear that pyrite Re-Os geochronology should use only unaltered pyrite from a single paragenetic stage of mineralization [18], which is difficult to achieve when 0.4 g of material is required for the analysis.

The use of Rb-Sr, Sm-Nd and Ar-Ar isotope systems for dating pyrite is limited by a number of isotope-geochemical reasons related to low concentrations of parental isotopes. The application of these methods is complicated by the fact that in the vast majority of the cases, the age is obtained for minerals (inclusions) whose direct genetic relationships with the ore-formation process are often difficult to establish [27–31].

Herein, we present a novel approach for dating pyrite by the U-Th-He method. The potential of this technique is verified on example of the Uzelga volcanogenic massive sulfide (VMS) deposit, South Urals [32,33]. The deposit is considered to be a standard of the Uralian-type VMS deposits [34,35] and has been a key for the development of a convective-hydrothermal model of VMS formation in the arc-related complexes of the Urals [36,37].

Similar to other VMS deposits, the Uzelga deposit is closely associated with coeval volcanic, volcaniclastic and sedimentary rocks [38–43] and volcano-sedimentary Fe (±Mn)-silica jasperites [44,45]. Therefore, it has an obvious stratigraphic age that coincides with the age of the host series [35,46–50] and represents a relevant case study to validate the accuracy of geochronological data.

2. Isotope-Geochemical Constrains

The U-Th-He method is based on the accumulation of He atoms produced by the alpha decay of U and Th. In the U-Th-He system, the chemical behavior of parent and daughter isotopes contrasts most significantly compared to other radioisotope systems. This provides unique opportunities for dating of processes not accessible by other techniques [51].

2.1. Uranium and Thorium in Sulfides

The concentration of U in sulfides varies over a wide range from few ppb to tens of ppm [17,52–54]. In uranium deposits, the concentration of U in pyrite can be as high as 2–4 wt.% [55]. The distribution of U in this mineral is highly heterogeneous [52]. In submarine hydrothermal sulfides, U usually strongly prevails over Th (Th/U = 0.001–0.04; [56]).

Pyrite can uptake U from aqueous solutions due to redox reaction with U (VI) on its surface [57,58]. The very low solubility of U under dominant reducing conditions of ore forming processes ensures that it remains fixed within the sulfide [52].

Inclusions of U-Th-bearing minerals can be another source of U and Th in sulfides [59,60]. Submicron inclusions of uraninite, brannerite, monazite, apatite, zircon and xenotime are reported for copper-zinc VMS ores [32,34,61–63]. The size of these inclusions, as a rule, does not exceed a few microns [64]. Alpha particles produced from the decay of U and Th travel relatively long distance away from their parents [65]. The mean U decay energy is ~5.4 MeV [65], which means the average

alpha-stopping distance in uraninite is ~10 μm (calculations in SRIM; [66]). Therefore, the radiogenic He produced in these inclusions mostly remains incorporated in the crystal lattice of the host pyrite.

Microradiographic studies have shown that for high-U sulfides, the inclusions of uraninite are more common. In low-U sulfides (<0.01%), neutron-induced fission tracks do not form radial patterns, which indicates a more homogeneous distribution of U, likely resulting from its adsorption during mineral growth [54].

2.2. Hydrothermal Fluid-Derived ^4He

Pyrite is known to be an ideal mineral for preserving He from an ore-forming fluid [67–70]. Typically, the concentration of trapped He in sulfides from black smokers in modern seafloor hydrothermal sulfide fields does not exceed 10^{-8}–10^{-10} cm^3 STP g^{-1} [71–75]. The amount of radiogenic ^4He depends on the U and Th content in pyrite and its age. The concentration of radiogenic ^4He in a 10-Ma old pyrite grain, which has 1 ppm U (Th/U = 0.001), is more than 10^{-6} cm^3 STP g^{-1}. Thus, the amount of fluid-derived ^4He may be considered insignificant for samples older than tens of millions of years. The younger grains of pyrite or those with lower U content, might require corrections for trapped He.

2.3. Retentivity of U-Th-He System in Pyrite and Mineral Stability

High-crystallinity pyrite has a particularly strong thermal retentivity for ^4He [11]. Step-heating experiments have shown that He begins to migrate from pyrite crystal lattice at temperatures of ~450–600 °C, when the mineral begins its transformation into pyrrhotite (under anoxic conditions). This indicates that there is likely no loss of He at temperatures of pyrite stability. High retention of He in pyrite is indirectly supported by the results of successful ^{190}Pt–^4He dating of sperrylite [8].

Pyrite is relatively fast oxidized under atmospheric or aquatic conditions [76]. However, under anoxic conditions pyrite has been shown to remain robust for billions of years even through post-mineralization thermal and metamorphic disturbances [77–79].

3. Object of Study

3.1. Geological Setting

The Uzelga deposit (54°07′ N, 59°20′ E) is one of the largest massive sulfide deposits of the Urals and contains about 4 Mt of Cu+Zn reserves. The deposit is located within the Verkhneuralsk ore district in the northern part of the East Magnitogorsk paleovolcanic belt (Figure 1) [32,37,80–82]. This belt comprises intra-oceanic arc-related complexes of Ordovician to Early Carboniferous ages [35,36,83–85].

The ore bodies of the deposit are mostly hosted by felsic, locally, altered rocks which form a large structure reminiscent of a volcanic dome (Figure 2). Primary volcanic structures are weakly deformed by small-amplitude faults. The ore-bearing basalt-rhyolite series belongs to the Upper Eifelian Karamalytash Formation and roughly corresponds to the *australis-kokelianus* zones [41], ca. 389 Ma [86]. The rocks are overlain by Givetian limestones, Lower Frasnian chert-siltstone horizon and Middle-Upper Frasnian volcano-sedimentary basalt-basaltic andesite unit [83]. The group of parallel WNW-trending subvolcanic mafic dikes of Givetian (?) age, which form thick (up to 20–30 m) steeply dipping bodies, cut the rocks of the Uzelga deposit [33,34].

Massive to semi-massive sulfide ores are located at two levels from the present surface, 130–380 m (bodies Nos. 1, 5, 6, 9) and 420–640 m (bodies Nos. 2–4, 7, 8) with 300–350 m between the levels (Figure 3). Ores are commonly slightly metamorphosed, retain relict syngenetic fabrics and they are considered as being close to primary ores that were deposited in seafloor [49] or seafloor/subseafloor [32–34,81,87] environments. The upper sulfide-bearing horizon is significantly enriched in tennantite-tetrahedrite, whereas the lower level is characterized by only a minor occurrence of tennantite and local enrichment in pyrrhotite (pyrite-pyrrhotite assemblage; ore body No. 4; Figure 3) [32,33,80,87].

The Uzelga deposit is an example of a long-lived, volcanic-related, seafloor/subseafloor ore-forming system [32,36,81,87–89]. The formation of main sulfide masses was synchronous with the Late Eifelian basalt-rhyolitic magmatism and was coeval with the terrigenous-carbonate sedimentation, ca. 389 Ma [34,35,40,41,44]. Hydrothermal processes remained active in the area throughout the Givetian stage, which is supported by—(i) the presence of disseminated sulfide mineralization in the Givetian limestones above the ore bodies of Uzelga deposit [35,37]; (ii) the position of ore body No 5, which is controlled by overlying limestones (Figure 3); (iii) the presence of large sulfide ore bodies (XIX Parts'ezda deposit) at 600 m distance within the Givetian rocks of the Ulutau Formation [80,90]. Sulfide mineralization is absent in the overlaying rocks, starting from the *puncata* zone [41,83], ca. 380 Ma [86]. Thus, the biostratigraphic age of ore mineralization of the Uzelga deposit is in a range of 389 to 380 Ma.

The VMS deposits of the Urals are subjected to varying degrees of later metamorphic events [34,91–93]. Ores of the Uzelga deposit mainly have massive textures. The common occurrence of colloform and breccias-like textures is evident of a low grade of post-depositional metamorphism [32,34,81] of prehnite-pumpellyite facies (~150–300 °C [93]). Zones of local recrystallization occur along rare steeply-dipping small-amplitude faults as well as in narrow (cm-dm thickness) contact zones of the mafic dikes. The largest area of ore recrystallization is located in the central part of the ore body 4 at the lower sulfide-bearing level corresponding to the occurrence of pyrrhotite-bearing ore on Figures 2 and 3.

The age of regional metamorphism is consistent within the Magnitogorsk zone and is significantly distinct from the age of island-arc volcanism and massive sulfide formation [33,85,93]. The Ar-Ar ages of sericite from the Babaryk (Alexandrinka district, Figure 1) and Barsuchi Log (~380 km to the South) VMS deposits are 340 ± 7 and 345 ± 3 Ma, respectively [94]. The same range of values ~350 Ma is measured for sericite from the Gai VMS deposit (~350 km to the SSW) by K-Ar isochron method [32].

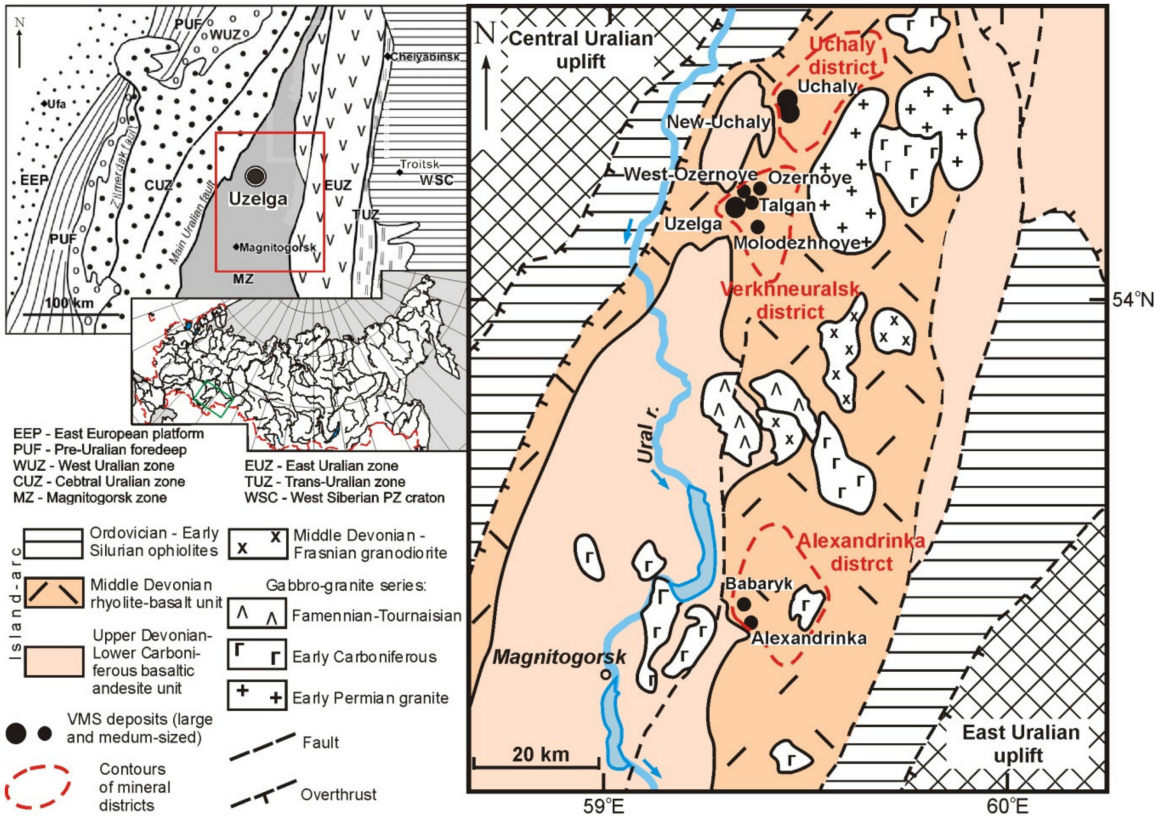

Figure 1. Schematic geological map of the Uchaly-Alexandrinka volcanogenic massive sulfide (VMS)-bearing area of the North Magnitigorsk zone, South Urals. Modified after [44]. The position of the Magnitogorsk zone in the structure of the South Urals is shown in the top left (modified after [98]).

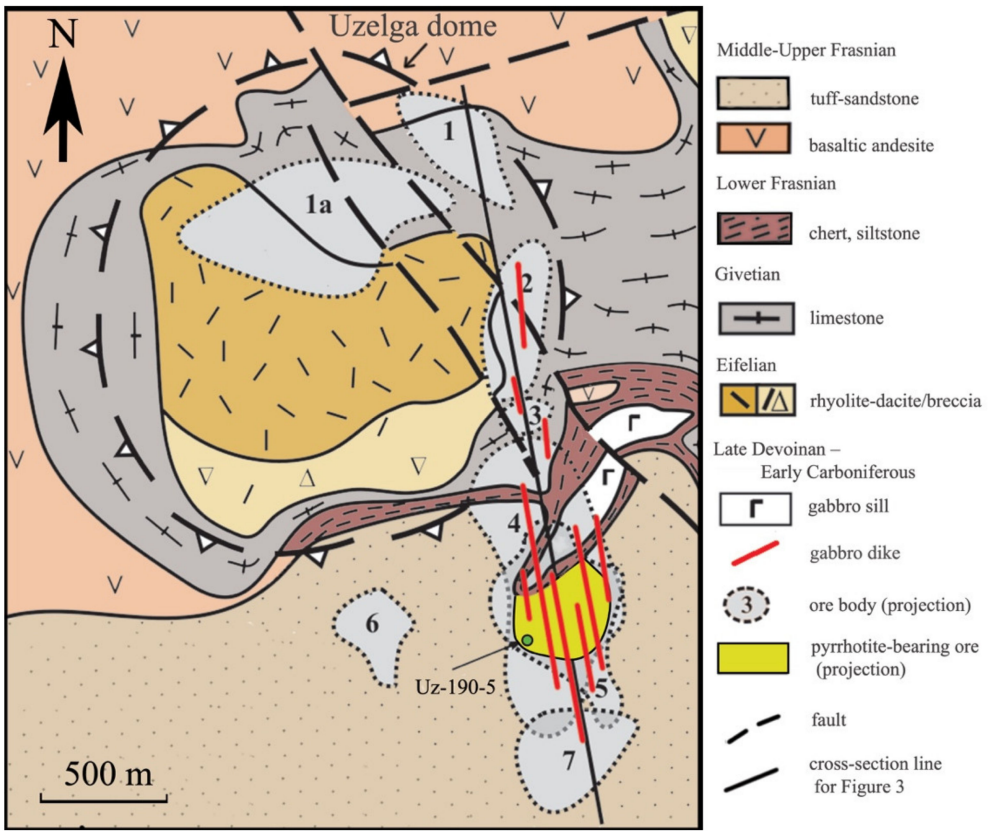

Figure 2. Geological map of the Uzelga deposit and position of the Uzelga volcanic dome, modified after [33].

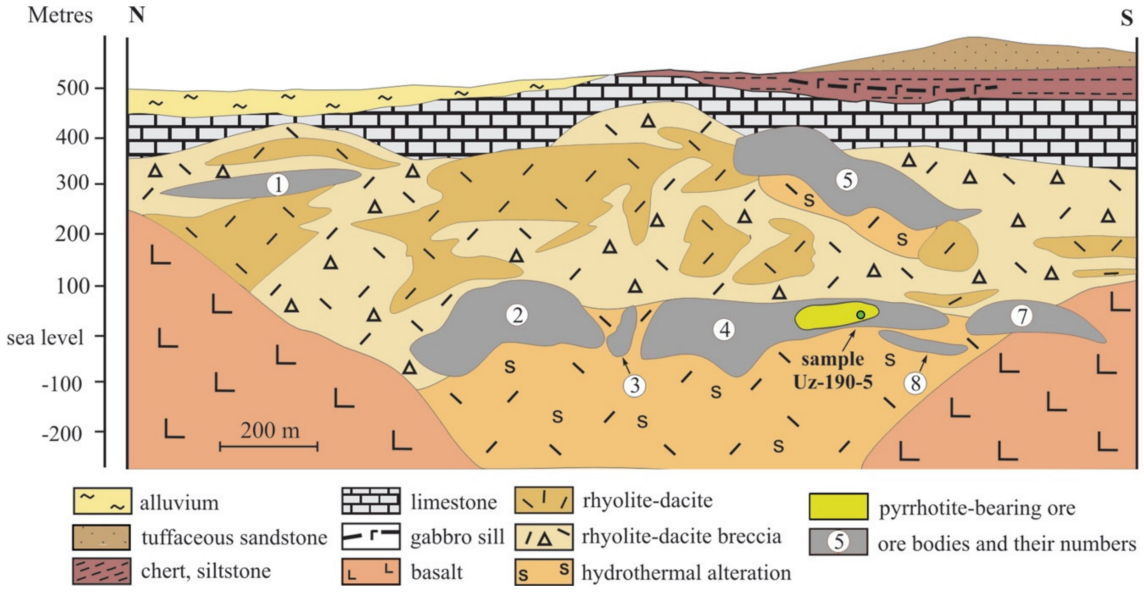

Figure 3. Longitudinal cross-section of the Uzelga deposit. Modified after [87,99] and underground mapping of the Uzelga mine.

Re-Os ages of sulfides from VMS ores of Urals are typically ~30 Ma younger than the ages of host rocks and show some consistent values ~360–365 Ma, that at the moment do not have generally accepted explanation [94,95]. Re-Os ages for sulfides of the Alexandrinka deposit (Alexandrinka district, Figure 1), which is the nearest to the Uzelga deposit dated by this method, is 355 ± 15 Ma [96].

No Re-Os data are available for the Uzelga deposit. The Pb-Pb isotope study of galena from VMS ores of the Urals was shown to be more useful for determining the source of the metals, rather than for the model Pb-Pb dating [97].

3.2. Ore Geochemistry and Mineralogy

Cu-Zn massive ore at the Uzelga deposit is dominant with following average range of contents: 1–1.5 wt% Cu; 2.5–5 wt% Zn, 0.8–2.5 ppm Au, 15–80 ppm Ag, 20–150 ppm Se; and 30–200 ppm Te [33,100,101].

Pyrite is the major ore mineral (50–95 vol%). Chalcopyrite (1–5, up to 10 vol%) and sphalerite (1–10, up to 30 vol%) are the major economic minerals. Tennantite-tetrahedrite is a common mineral in both the lower (0.1–1 vol%) and upper (0.5–5 vol%) sulfide lenses. Galena occurs widely but in smaller amounts (0.1–0.5 vol%). Pyrrhotite is abundant in the lower ore-bearing level and comprises the considerable fragments in the central zone of ore body No. 4 (Figures 2 and 3). Two massive ore types are dominant at the lower ore-bearing level—pyrite-sphalerite-chalcopyrite (minerals listed in decreasing abundance order) and a pyrrhotite-pyrite-sphalerite-chalcopyrite. The latter is dominant by pyrite-pyrrhotite (±sphalerite, ±chalcopyrite, ±siderite) assemblage.

By the beginning of the 21st century, the reserves of the Uzelga deposit were about 84 billion tons at an average Cu content of 1.36 wt.% and Zn content of 3.4 wt%, corresponding to about 1.1 Mt Cu and 2.8 Mt Zn [33].

3.3. Sample Location and Description

Pyrite grains for U-Th-He dating were manually extracted from a large (25 × 25 cm) specimen of pyrrhotite-pyrite-sphalerite-chalcopyrite ore of the lower horizon (sample Uz-190-5, level –550 m) in the southern part of ore body No. 4 (Figures 2 and 3). The ore is characterized by a porphyry-like texture, marked by large, up to 5–8 cm, pyrite porphyroblasts enclosed in a fine-grained ground mass of pyrrhotite, minor sphalerite and rarer chalcopyrite (Figure 4). According to instrumental neutron-activation analyses (INAA), pyrite (sample Uz-190-5) is rich in Se (498 ppm), Co (357 ppm) and Te (117 ppm) and has lower contents of As (<1 ppm), Ag (<1 ppm), Sb (<0.3 ppm) and Au (0.2 ppm), comparing to typical pyrite of this deposit [33,101].

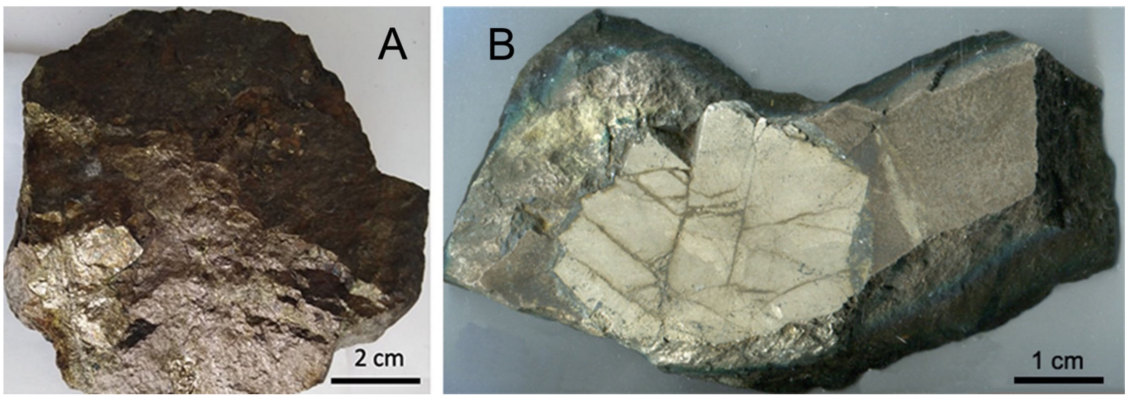

Figure 4. Macrophotographs of the fragments of pyrrhotite-pyrite-sphalerite-chalcopyrite ore of the lower horizon (sample Uz-190-5, level −550 m) in the southern part of ore body No. 4 (Figures 2 and 3). There are a few large porphyroblasts of pyrite in the left bottom part of the photograph (**A**) and large polycrystalline pyrite porphyroblast in pyrrhotite-dominated ore (**B**).

4. Analytical Methods

Prior to U-Th-He dating, pyrite grains in polished sections were studied on a Hitachi S-3400N scanning electron microscope equipped with an AzTec Energy 350 detector ("Geomodel" Research Centre, Saint-Petersburg State University). Grain crystallinity was studied using a Bruker D2 PHASER

powder diffractometer, ($CuK_{\alpha 1+2}$ radiation, 30 kV/15 mA, 2theta degree step 0.02, count time for each step 0.6 s) (Research Centre for X-ray Diffraction Studies, Saint Petersburg State University). The data were processed using Rietveld refinement in TOPAS.

Thermal analysis of pyrite was undertaken using a NETZSCH STA 449 F3 Jupiter thermal analyzer (Department of Geochemistry, Saint-Petersburg State University, St Petersburg, Russia), which allows simultaneous measurement of the mass loss (thermogravimetric analysis, TG and DTG) and thermal effects (differential scanning calorimetry, DSC).

The fragments of pyrite grains 0.5–1.5 mg in weight were selected for U-Th-He dating. Following the recommendations of Reference [18], part of the grains were washed in 0.2 N HCl in an ultrasonic cleaner for 30 min to remove possible alteration phases. The concentrations of U and Th in the leached material were monitored with an ELEMENT XR ICP mass-spectrometer (Vernadsky Institute of Geochemistry and Analytical Chemistry, Russian Academy of Sciences). Prior and after leaching, the samples were weighted on a Sartorius RC 210 P balance.

4.1. Measurement of Radiogenic ^{4}He Contents

The ^{4}He contents were measured at the Institute of Precambrian Geology and Geochronology, Russian Academy of Sciences (IPGG RAS) with a high-sensitivity MSU-G-01-M mass spectrometer. For extraction of He, we used original methodological approach, that excludes U and Th loss during annealing. The pyrite grains and their fragments ~0.5–1 mg in weight were placed in a quartz ampoule (~1 cm long) and sealed under vacuum conditions (10^{-3} torr) (Figure 5A). Using a special lock, the ampoule was transported into a Re cylinder and heated in several steps up to temperatures of ~1100 °C. When heated, He easily diffuses through thin walls of the ampoule, while U and Th remain inside. This approach avoids contamination of the sample with the material of the extractor of the mass spectrometer and also saves the sample for further determination of U and Th. Details of the He measurement technique and the design of the instrument are described in References [5,102]. The complete procedural blank determined by heating the empty ampoule in the Re cuvette to 1100 °C corresponds to ~5×10^{-10} cm^3 STP, whereas the detection limit of the instrument is ~5×10^{-13} cm^3 STP of ^{4}He. After the extraction of He, the ampoule was removed from the mass spectrometer for subsequent separation of U and Th (Figure 5b).

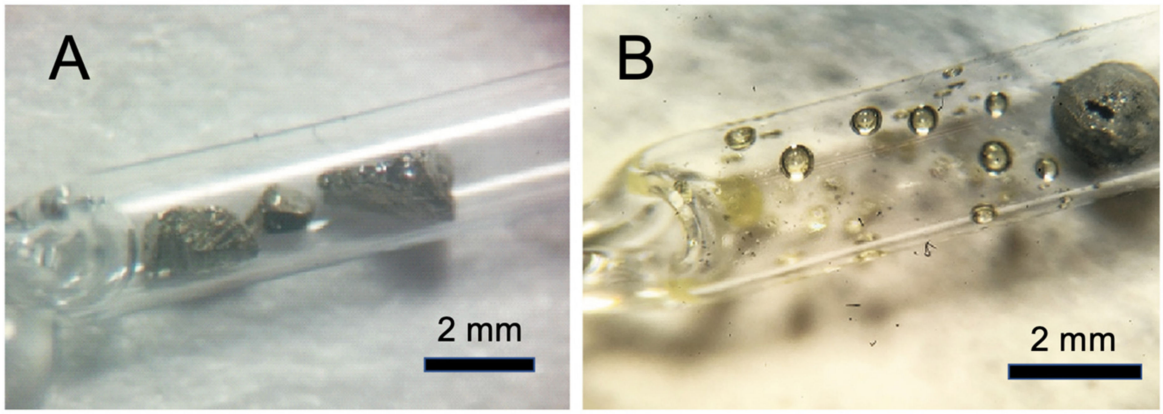

Figure 5. (**A**) Pyrite grains in quartz ampoule before He extraction; (**B**) products of thermal decomposition of pyrite grains after annealing in sealed quartz ampoule at temperature ~1100 °C.

The possibility of simple wrapping of pyrite grains in Ta foil for the extraction of He was also tested. The procedure is easier and the blank level is around five times lower that using quartz ampoule. In this case, if the U and Th are mainly preserved in the form of inclusions, then evaporation of S during heating in the extractor should not lead to loss of parent nuclides. The methodology of He extraction and U and Th analysis remained the same.

4.2. Measurement of U and Th Contents

The U and Th contents were measured by isotope dilution method. The quartz ampoule was opened and spiked with a combined ^{230}Th–^{235}U tracer. The samples were dissolved in closed Teflon vials for 24 h at a temperature of 130 °C in concentrated nitric acid. The products of the thermal decomposition of pyrite (Figure 5b) include sulfur, alpha-iron, pyrrhotite and troilite (X-ray diffraction (XRD) analysis). All these components are dissolved in concentrated nitric acid [103]. As was discussed previously, some part of U and Th in sulfides might occur in submicron-sized mineral inclusions, which probably does not dissolve in nitric acid. The dissolution of pyrite yields sulfuric acid, which enhances the dissolution of the submicron-sized inclusions of U and Th-bearing minerals [103]. The completeness of dissolution was monitored using an optical microscope. The ^{235}U/^{238}U and ^{230}Th/^{232}Th isotope ratios were measured on an ELEMENT XR ICP mass-spectrometer (Vernadsky Institute of Geochemistry and Analytical Chemistry).

4.3. Calculation of U-Th-He Age

Because of dating the fragments of larger grains, the calculation of U-Th-He ages requires no alpha-recoil corrections [65]. The amount of radiogenic ^{4}He accumulated in the mineral over the time t is:

$$^{4}He = 8\,^{238}U\left(e^{\lambda_{238}t}-1\right)+7^{235}U\left(e^{\lambda_{235}t}-1\right)+6^{232}Th\left(e^{\lambda_{232}t}-1\right), \quad (1)$$

where λ_{238}, λ_{235} and λ_{232} are the decay constants of ^{238}U, ^{235}U and ^{232}Th, respectively. This equation has no analytical solution relative to t but easily be solved iteratively [104] and several options for approximate calculations exist that are remarkably accurate for all applications [105].

The average U-Th-He age can be calculated in different ways [104]—(1) arithmetic mean of the single-grain ages; (2) the "pooled" age; (3) the U-Th-He isochron age; and (4) the central age (HelioPlot; [106]). From the mathematical viewpoint, the latter method is the most accurate [104].

The accuracy of complete dating procedure (measurement of He, U and Th) was assessed by simultaneous experiments on the Durango apatite, which is the international standard for U-Th-He method. The calculated central age for five grains of Durango apatite is 32.2 ± 1.9 (2σ) Ma (MSWD 1.57), which is in good agreement with published data of 32.3 ± 0.9 Ma [107] (Table 1).

Table 1. Results of U-Th-He dating of pyrite from Uzelga deposit and Durango apatite.

Sample ID	Weight, (mg)	^{4}He, cm^{3} STP g^{-1}	U, 10^{10} at	σ	Th, 10^{10} at	σ	^{4}He, 10^{10} at	σ	T, Ma	σ
Uzelga pyrite										
599	0.84	1.06×10^{-4}	510	75	1.6	1.1	239	7	350	50
600	0.35	4.01×10^{-5}	70.0	1.4	1.7	1.1	37.4	1.2	399	15
601	0.81	1.55×10^{-4}	680	120	1.1	0.7	336	9	370	60
602	0.49	2.07×10^{-4}	550	44	0.8	0.4	271	7	370	30
603	0.28	1.20×10^{-4}	178	13	1.5	1.1	90.6	2.5	380	29
604	0.69	1.70×10^{-4}	580	50	2.3	1.2	316	8	410	36
631	–	–	154	8	1.5	0.7	75	3	366	24
632	–	–	58	3	60	30	266	6	2370	170
633	–	–	1340	70	4	2	667	17	375	20
676 [1]	–	–	13.85	0.08	5.0	2.7	27	1	1240	58
677 [1]	–	–	10.52	0.03	3.3	1.7	26	1	1550	58
433	–	–	880	50	12.9	0.8	476	2	404	22
435	–	–	38	2	10.3	0.6	20	1	371	21
437	–	–	15	1	5.2	0.3	10	1	446	27
							Central age [2]:		382	6

Table 1. *Cont.*

Sample ID	Weight, (mg)	^{4}He, cm^3 STP g^{-1}	U, 10^{10} at	σ	Th, 10^{10} at	σ	^{4}He, 10^{10} at	σ	T, Ma	σ
Durango apatite										
660	–	–	1700	55	39,500	1200	412	8	29.6	0.6
661	–	–	2030	170	43,800	3400	434	9	27.8	0.6
662	–	–	850	60	17,000	1300	187	4	30.2	0.6
663	–	–	1240	60	29,000	1400	334	7	32.4	0.7
666	–	–	554	17	12,300	300	160	4	36.6	0.9
							Central age:		32.2	1.0
Qu blank	–	–	1.26		0.52		1.23			
Ta blank	–	–	1.52		1.56		0.31			

[1] in Ta foil; [2] samples 676, 677, 632 and 437 were excluded from the calculation of the central age; at—atoms; T—age; "–" – has not been measured.

In total, we dated 14 fragments of pyrite with weights ranging from 0.5 to 1.5 mg (including nine earlier values [12]). Two pyrite grains were wrapped in Ta foil and others were sealed in the quartz ampoule (Table 1). The U-Th-He ages of each grain were calculated in HelioPlot software [106].

5. Results

5.1. Mineralogical Features

Scanning electron microscopy (SEM) analysis of the pyrite grains revealed the presence of micron-sized inclusions of uraninite, which are spatially associated with chalcopyrite veinlets (Figure 6). Rare inclusions of sphalerite, hematite, altaite, chromite and native gold are also observed within the grains.

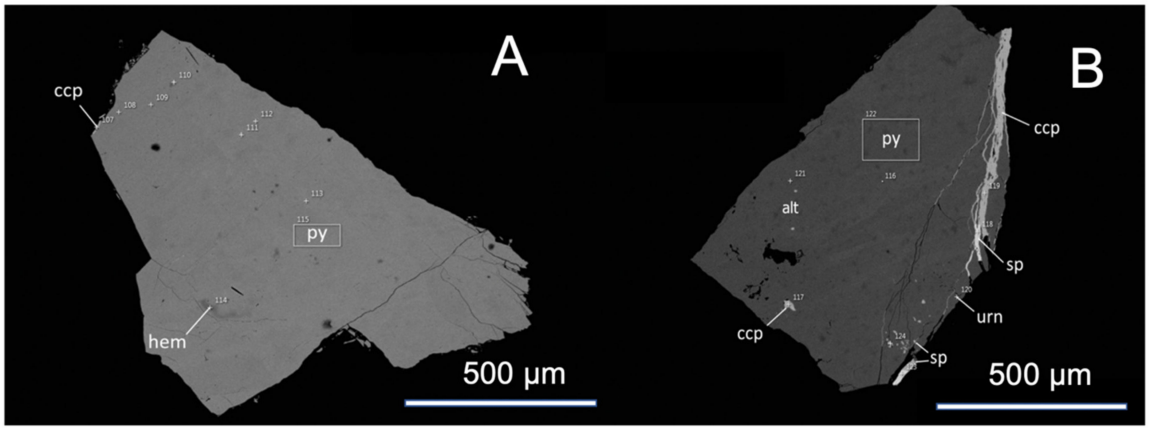

Figure 6. Scanning electron microscopy (SEM) images of selected pyrite grains from the Uzelga deposit. py—pyrite (FeS_2), ccp—chalcopyrite ($CuFeS_2$), hem—hematite (Fe_2O_3), sp—sphalerite (ZnS), alt—altaite (PbTe), urn—uraninite (UO_2). (**A**) pyrite with minor hematite; (**B**) pyrite with tiny inclusions of altaite, sphalerite and chalcopyrite as well as sphalerite-chalcopyrite veinlet (with associated uraninite).

XRD analysis showed that pyrite is characterized by high crystallinity—the size of the regions of coherent scattering (crystallite size) is more than the resolution of the diffractometer, which is 9000 nm.

Thermal analysis showed no thermal effects (the absence of oxidation or sulfur release) within the temperature range 25–400 °C, which indicates the high degree of stoichiometry of pyrite (Figure 7). No thermal effects that might be associated with the decrepitation of fluid inclusions were also observed.

Three exothermic effects at the DSC curve at 480.3, 552.2–568.5 and 612.0 °C, were accompanied by mass loss, as indicated by the TG and DTG curves. The first two effects correspond to the breakdown of pyrite to pyrrhotite and magnetite [108,109]. The third effect may correspond to the decomposition of sphalerite inclusions [110].

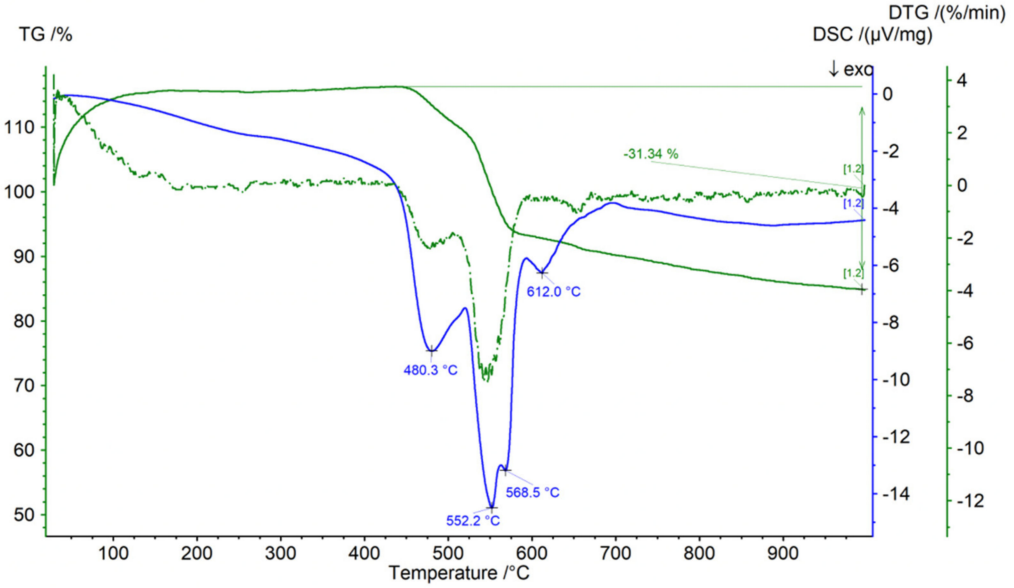

Figure 7. Results of comprehensive thermal analysis of pyrite from the Uzelga deposit within a temperature interval of 25 to 1000 °C in the atmosphere. DTA (differential thermal analysis)—solid blue line; TG (termogravimetry) —solid green line; DTG (derivative termogravimetry) —dotted green line. Heating rate—20K/min. Sample weight is ~10 mg.

5.2. Results of Leaching Experiments

Fragments of pyrite grains lost 0.2%–0.3% of their weight after 30 min washing in 0.2 N HCl in an ultrasonic cleaner (Table 2). The Th content of the solution was low and typically did not exceed three times the blank level. The amount of U leached to the solution was remarkably higher, up to 57 ng. The leached grains were considered unsuitable for U-Th-He dating, as they have lost part of U.

Table 2. U and Th contents of the solution after washing of pyrite grains from the Uzelga deposit in 0.2 N HCl for 30 min in ultrasonic cleaner.

Num	Weight, mg	σ,%	Δ, mg	σ,%	Th, ng	Th, ppm	±	U, ng	U, ppm	±	Th/U
1	1.217	0.2	0.003	100	b.d.l.			0.23	80	80	
2	0.751	0.4	0.003	100	b.d.l.			0.03	10	10	
3	32.247	0.0	0.057	5	0.037	0.65	0.03	56.96	1000	50	0.0006
4	1.954	0.2	0.006	50	0.001	0.16	0.08	11.38	1900	950	0.0001
5	3.307	0.1	0.023	13	b.d.l.			6.50	280	40	
6	1.358	0.2	0.002	150	b.d.l.			0.39	200	300	
bl					0.001			0.001			

Num – sample number; bl—blank; Δ —difference in sample weight before and after leaching.

5.3. U-Th-He Dating Results

The concentrations of ^{4}He in pyrite grains were ~4×10^{-5}–2×10^{-4} cm^3 STP g^{-1}. From all samples, He was released at temperature of their decomposition into pyrrhotite and sulfur (~500 °C). The concentrations of U varied from 0.8 to 5 ppm. The average Th/U ratio was ~0.007.

Most samples ages in a range 350–410 Ma (Table 1). Two samples of pyrite (#676 and #677) that were wrapped in Ta foil gave remarkably older ages (1240–1550 Ma). They also showed very low concentrations of U (~50 ppb) and higher Th/U ratios (~0.3). This suggests loss of U during annealing of grains from an unsealed Ta envelope. Thus, these grains were ignored from calculation of the average (central) U-Th-He age. Pyrite grain #632 also gave an older age of ~2370 Ma and showed a very low concentration of U (~200 ppb) and atypically high Th/U ratio of 1. This anomalous grain was also excluded from the calculations, as well as grain #437 with very low ^{4}He content.

The central age calculated for ten grains of pyrite is 382 ± 12 (2σ) Ma. The arithmetic mean is 386 ± 18 (MSWD 0.42) and the geometric mean is 387 ± 18 (MSWD 0.42). Ternary and log-ratio plots are not informative due to the low concentration of Th. Therefore, for visualization of the data, we plotted an U-Th-He isochron (Figure 8).

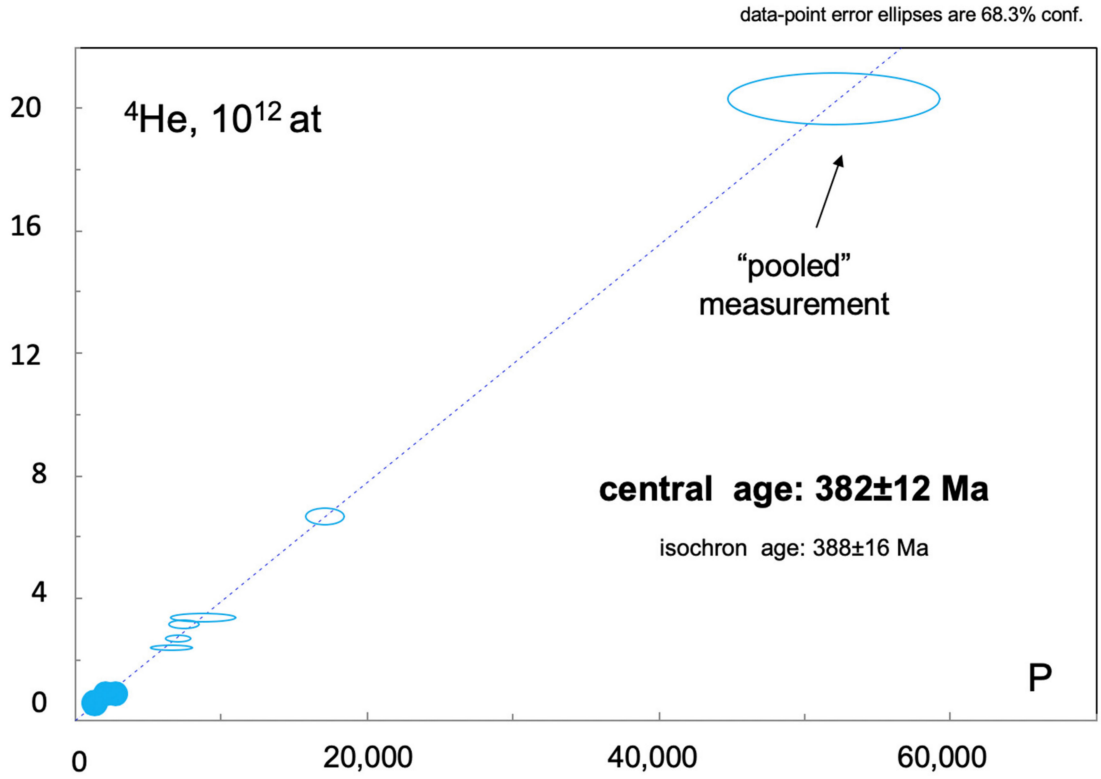

Figure 8. Linearized U-Th-He diagram for pyrite from the Uzelga deposit. According to the linear age equation, the U-Th-He age is given by the slope of the regression line; the "pooled" age is a "synthetic multi-grain age" calculated from the summed production rates and helium-abundances of all the measurements [104]. Uncertainty represents 2 σ. Solid circles indicates grains, which uncertainty envelope is too small to be visualized. Isochron age is calculated in Isoplot Excel add-on from a regression line [111].

6. Discussion

The central age of 382 ± 12 Ma for pyrite from the Uzelga deposit is consistent with independent (biostratigraphic) estimations of the age of ore formation (ca, 389–380 Ma) and is remarkable older than the age of regional prehnite-pumpellyite facies metamorphism (~340–345 Ma; see Section 3.1). The pyrite U-Th-He ages are quite reproducible but show scattering in a range 350–410 Ma, which can have different explanations: (i) the presence of excess ^{4}He; (ii) the loss or input of U, Th, He during geological history; (iii) methodological imperfections.

6.1. Excess ^{4}He

There are several reasons of ^{4}He excess in minerals: (i) trapped hydrothermal ^{4}He; (ii) inclusions-related excess of ^{4}He; (iii) implanted radiogenic ^{4}He.

6.1.1. Trapped Hydrothermal ^{4}He

The concentrations of He in submarine hydrothermal fluids are 10^{-6} to 10^{-5} cm^3 STP ^{4}He g^{-1} [112]. Modern submarine hydrothermal sulfides typically yield 10^{-8}–10^{-10} cm^3 STP ^{4}He g^{-1} [71]. Helium concentrations in them do not show any relationship with geodynamic settings (fast/slow spreading mid ocean ridge; back-arc basin) or water depth [113]. There is no correlation between concentration of trapped He and its isotopic composition [113,114]. The study of He in modern massive sulfides from Middle Valley which are mainly deposited at the subseafloor environment (Ocean drilling program Leg 139, Site 856) show the same range of He concentrations [114].

The measured concentrations of ^{4}He in pyrite from the Uzelga deposit are several orders of magnitude higher (10^{-4}–10^{-5} cm^3 STP g^{-1}) than the concentrations of He that is trapped by modern hydrothermal sulfides. Thus, if we assume that the pyrite had trapped the fluid with the same proportion as modern ocean sulfides the contribution of fluid-derived helium can be considered insignificant.

Studied pyrite porphyroblasts is a product of interaction of primary ores of the lower level with later high-temperature hydrothermal fluids, that might be enriched in He. By the moment the highest measured concentration of trapped He in sulfides is that in arsenopyrite from the Panasqueira deposit (1.2 10^{-6} cm^3 STP g^{-1}; [69]). The Panasqueira deposit is not a VMS type deposit, however, if we assume that concentration of trapped He in the pyrite-pyrrhotite assemblage of the Uzelga deposit is within the same range as in arsenopyrite from the Panasqueira deposit, the contribution of trapped component in the total balance of ^{4}He would not exceed 3%.

6.1.2. Inclusions-Related Excess of ^{4}He

Primary ores were precipitated in the seafloor environment as well as in subseafloor position—beneath weakly lithified calcareous, siliceous and silty sediments inside of felsic volcanic unit [81,87,115–118]. Thus, they had a chance to trap some relatively large (>30 μm) minerals inclusions (zircon, rutile, etc.), that had already accumulated some ^{4}He. The studied samples were derived from the pyrrhotite + pyrite (±sphalerite, chalcopyrite, siderite) ores that were formed at the latest stage of hydrothermal process at 300–400 °C (up to 520 °C [32]). This temperature is far above than closure temperature of U-Th-He system in most U and Th-bearing minerals (70–250 °C) [51]. Thus, it is very unlikely that any ^{4}He remains inside the trapped mineral inclusions.

6.1.3. Implanted Radiogenic ^{4}He

It is difficult to estimate the amount of alpha-particles generated within the fragments of pyrite grains that have been ejected and implanted as the distribution of U and Th in pyrite appears to be heterogeneous (see Section 2.1) [65]. The diameter of the studied pyrite grains (~300–800 μm) are remarkably larger than alpha-stopping distance in pyrite, which is ~18 μm (SRIM [66]). Thus, the fraction of implanted ^{4}He, relative to retained ^{4}He might be considered as insignificant [65].

6.2. U-Th-He System Behavior in Pyrite

The open behavior of the U-Th-He system can be related to the He loss, U, Th input or U and Th loss. The first two processes lead to relatively younger U-Th-He ages, when the last one tends to increase the age value.

6.2.1. Uranium and Thorium in Pyrite

The concentrations of U and Th in pyrite grains from the Uzelga deposit (0.8 to 5 ppm) are within the range typical of sulfides from modern black smokers (0.00–11 ppm; [17,52–54]). Uranium strongly

prevails over Th, which is consistent with its inferred hydrogenic origin [52]. SEM analysis of pyrite grains show that part of U is associated with micron-sized inclusions of uraninite that are spatially related to chalchopyrite veinlets (Figure 6b). The size of the inclusions is small enough (<10 μm) so that all He produced in them is implanted into pyrite due to alpha-recoil effect (see Section 2.1).

The apparent 'aging' of pyrite grains that were annealed in the Ta foil indicates a loss of U during heating. Uraninite is a highly refractory compound. At 1300 °C, the UO_2 vapor pressure is negligible (~1.6×10^{-8} torr). Thus, it is unlikely that heating the sample to 1100 °C could lead to significant loss of U from uraninite inclusions. More likely, part of U occurs in absorbed form within pyrite grains.

Surprisingly, washing of pyrite grains in 0.2 N HCl led to leaching of a significant amount of U (Table 2). Simple calculations allow us to estimate that the concentration of U in dissolved material reaches 1–2%, with a Th/U ratio of ~0.003. The 0.2 N HCl solution is a very weak acid that can mainly dissolve alteration phases or probably some carbonates [103]. However, it is highly unlikely that the concentration of U in any associated carbonate could be as high as 1000 ppm, as oceanic carbonates have up to 2 ppm U [119]. Among U-rich minerals, amorphous uranium oxides are the most soluble. Thus, due to the radiation damage, the zones around U-rich inclusions in pyrite and uraninite itself probably became highly defective, metamict and therefore easily dissolved. Mobilization of U is crucial for retentivity of U-Th-He system in pyrite as it indicates that even at the room temperatures U can be washed out from pyrite grains by weak acid solutions. This phenomenon requires additional study.

6.2.2. Radiogenic ^{4}He in Pyrite

Radiogenic He released from the studied samples at the temperatures of pyrite decomposition (>450 °C). All grains gave U-Th-He age that is remarkably older than the age of a regional metamorphic event (~340–345 Ma; see Section 3.1). This indicates high retention of radiogenic He in pyrite during the prehnite-pumpellyite facies metamorphism (150–300 °C) which is in a good agreement with kinetic experiments [11]. There is still some probability that He loss occurred simultaneously with U loss, which may explain the absence of younger ages. Taking into account the reproducible U-Th-He ages and contrast geochemical behavior of He, U and Th, it seems to be very unlikely.

6.3. Methodological Imperfections

The main methodological disadvantages that could lead to scattering of U-Th-He ages are incomplete release of He from pyrite grains and its incomplete decomposition. The temperature of ^{4}He release from the grains was ~1100 °C. That is more than enough to release all He from pyrite grains [11]. The pyrite grains were dissolved in no HF acid (see Section 4.2), as we tried to avoid the dissolution of fragments of the quartz ampoule. Although we registered no undissolved mineral inclusions in the vials after the treatment the sample by HNO_3 acid, some small silicate U,Th-bearing inclusions might remain undissolved. Likely it is the case of the grain #632 that gave remarkably older age.

6.4. Comparison of Pyrite U-Th-He and Geological Ages

The age value of 382 ± 12 Ma without error for pyrite from the Uzelga deposit tend to the lower boundary of the biostratigraphic age interval 389–380 Ma.

The pyrrhotite-bearing ore (ore body No 4; Figures 3 and 4) with studied pyrite porphyroblasts is a product of interaction of early ores of the lower level with high-temperature hydrothermal fluids that formed upper sulfide-bearing horizon (ore body No 4 is situated just beneath ore body No 5; Figures 2 and 3) [32,34]. Pyrite porphyroblasts were formed due to retrograde desulfurization of pyrrhotite [115,120]. Spatial association of uraninite with chalcopyrite veinlets, which cross-cut the pyrite porphyroblasts, indicates that the age likely reflects the final stage of synvolcanic ore formation.

7. Conclusions

The possibility of U-Th-He dating of pyrite is shown on example of high-crystallinity stoichiometric pyrite from the Uzelga VMS deposit, South Urals. The U-Th-He age without error for ten pyrite fragments from a large specimen of pyrite-pyrrhotite massive ore of 382 ± 12 Ma (2σ) is in agreement with biostratigraphic age estimations of ore-bearing hydrothermal activity (389–380 Ma).

In general, single-grain U-Th-He ages tend to suffer from overdispersion with respect to the formal analytical precision [121]. Thus, reliable U-Th-He dating require a set of analyses (multi single aliquot dating). The U-Th-He dating has certain obvious limitations. Very small grains (less than 200 μm) will lose a large percentage of He due to the alpha-recoil effect. This problem is solved by introducing an additional mathematical correction but it greatly increases the uncertainty of measurements [121]. Grains that are younger than tens of millions of years or have relatively low U content (<100 ppb) should require additional corrections on trapped fluid-derived ^{4}He. Sample preparation seems to be very important for accurate He dating. Routine prewashing of grains in 0.2 N HCl is not suitable for the removal of possible alteration phases, as it can also mobilize U. Development of new protocols are required. Nevertheless, the U-Th-He dating technique is rather promising, as it allows to date single pyrite grains (~500 μm).

Several theoretical problems should be solved to make this technique widely acceptable. Will it be possible to date non-stoichiometric pyrite, since it is much less stable? Does recrystallization completely reset the U-Th-He system? It is unclear how trace elements (i.e., As, Co, Ni, Au, etc.) affect the retentivity of He in the pyrite. It is also unclear if the zonation of pyrite affects the age values and whether the rims can differ significantly in age. The problem of the behavior and preservation of U in pyrite remains open. The relative ease of U-Th-He dating in comparison with other geochronological methods and small amount of the material (~0.5–1 mg) required for this dating technique makes this approach interesting for further development.

Author Contributions: Methodology and investigation, O.Y., M.P., A.K. and I.V. Field work and sampling, I.V. Writing – original draft preparation, O.Y. and I.V. Reviewed and edited the draft, O.Y., M.P., A.K., E.F. and I.V. Discussion, O.Y., M.P., A.K., E.F. and I.V. Project leadership and administration, O.Y and A.K. All authors have read and agreed to the published version of the manuscript.

Funding: The Russian Scientific Foundation, project no. 19-77-00097 (application of the U-Th-He method to the direct dating of pyrite, methodological approach for measurement of U, Th and He, scanning electron microscope, XRD, ICP-MS study and thermal analysis), Ministry of Science and Higher Education of the Russian Federation (field work, sampling and INAA study - research program of the Institute of Geology of Ore Deposits, Petrography, Mineralogy and Geochemistry (IGEM) RAS; sample preparation—under state contract No. 0153-2019-0002 of Institute of Precambrian Geology and Geochronology RAS) and the Russian Foundation for Basic Research, project no. 20-05-00849 (geological-genetic interpretation) funded this research.

Acknowledgments: We would like to thank geological staffs of the Uralian Mining and Metallurgical Company (Uzelga Mine) and personally Yuri Avilovich for assistance during field work and two anonymous reviewers for the constructive comments.

Conflicts of Interest: The authors declare no conflict of interest.

References

1. Farley, K.A. (U-Th)/He Dating: Techniques, Calibrations and Applications. *Rev. Mineral. Geochem.* **2002**, *47*, 819–843. [CrossRef]
2. Schmitt, A.K.; Danisik, M.; Evans, N.J.; Siebel, W.; Kiemele, E.; Aydin, F.; Harvey, J.C. Acigol Rhyolite Field, Central Anatolia (Part 1): High-Resolution Dating of Eruption Episodes and Zircon Growth Rates. *Contrib. Mineral. Petrol.* **2011**, *162*, 1215–1231. [CrossRef]
3. Vasconcelos, P.M.; Heim, J.A.; Farley, K.A.; Monteiro, H.; Waltenberg, K. ^{40}Ar/^{39}Ar and (U-Th)/He—^{4}He/^{3}He Geochronology of Landscape Evolution and Channel Iron Deposit Genesis at Lynn Peak, Western Australia. *Geochim. Cosmochim. Acta* **2013**, *117*, 283–312. [CrossRef]

4. Shukolyukov, Y.A.; Yakubovich, O.V.; Yakovleva, S.Z.; Sal'nikova, E.B.; Kotov, A.B.; Rytsk, E.Y. Geothermochronology Based on Noble Gases: III. Migration of Radiogenic He in the Crystal Structure of Native Metals with Applications to Their Isotopic Dating. *Petrology* **2012**, *20*, 1–20. [CrossRef]
5. Shukolyukov, Y.A.; Yakubovich, O.V.; Mochalov, A.G.; Kotov, A.B.; Sal'nikova, E.B.; Yakovleva, S.Z.; Korneev, S.I.; Gorokhovskii, B.M. New Geochronometer for the Direct Isotopic Dating of Native Platinum Minerals (190Pt-4He Method). *Petrology* **2012**, *20*, 491–505. [CrossRef]
6. Yakubovich, O. New 190Pt-4He Method of Isotope Geochronology for Dating Minerals of Platinum. Ph.D. Thesis, Saint Petersburg University, St Petersburg, Russia, 2013; p. 126.
7. Mochalov, A.G.; Yakubovich, O.V.; Bortnikov, N.S. ^{190}Pt–^{4}He Age of PGE Ores in the Alkaline–Ultramafic Kondyor Massif (Khabarovsk District, Russia). *Dokl. Earth Sci.* **2016**, *469*, 846–850. [CrossRef]
8. Yakubovich, O.V.; Mochalov, A.G.; Sluzhenikin, S.F. Sperrylite (PtAs2) as a ^{190}Pt–^{4}He Geochronometer. *Dokl. Earth Sci.* **2015**, *462*, 88–90. [CrossRef]
9. Campbell, I.H.; Czamanske, G.K.; Fedorenko, V.A.; Hill, R.; Stepanov, V. Synchronism of the Siberian Traps and the Permian-Triassic Boundary. *Science* **1992**, *258*, 1760–1764. [CrossRef]
10. Cabri, L.J.; Stern, R.A.; Czamanske, G.K. Osmium Isotope Measurements of Pt-Fe Alloy Placer Nuggets from the Konder Intrusion Using a SHRIMP II Ion Microprobe. In Proceedings of the 8th International Platinum Symposium, Johannesburg, South Africa, 28 June–3 July 1998; pp. 55–58.
11. Yakubovich, O.V.; Gedz, A.M.; Vikentyev, I.V.; Kotov, A.B.; Gorokhovskii, B.M. Migration of Radiogenic Helium in the Crystal Structure of Sulfides and Prospects of Their Isotopic Dating. *Petrology* **2019**, *27*, 59–78. [CrossRef]
12. Yakubovich, O.V.; Vikentyev, I.V.; Zarubina, O.V.; Bryanskiy, N.V.; Gorokhovskii, B.M. U-Th-He Dating of Pyrite from the Uzelga Copper-Zinc Massive Sulfide Deposit (South Urals, Russia): First Application of a New Geochronometer. *Dokl. Earth Sci.* **2019**, *485*, 368–371. [CrossRef]
13. Bowles, J.; Howie, R.; Vaughan, D.J.; Zussman, J. Non-Silicates, Oxides, Hydroxides and Sulphides. In *Rock-Forming Minerals*; The Geological Society: London, UK, 2011; p. 920.
14. Rusinov, V.L. *Metasomatic Processes in Volcanic Rocks*; Nauka: Moscow, Russia, 1989.
15. Zharikov, V.A.; Pertsev, N.N.; Rusinov, V.L.; Callegari, E.; Fettes, D.J. Metasomatism and Metasomatic Rocks. In *Recommendations by the IUGS Subcommission on the Systematics of Metamorphic Rocks: Web Version 01.02.07*; British Geological Survey: Nottingham, UK, 2007.
16. Craig, J.R.; Vokes, F.M.; Solberg, T.N. Pyrite: Physical and Chemical Textures. *Miner. Depos.* **1998**, *34*, 82–101. [CrossRef]
17. Large, R.R.; Halpin, J.A.; Danyushevsky, L.V.; Maslennikov, V.V.; Bull, S.W.; Long, J.A.; Gregory, D.D.; Lounejeva, E.; Lyons, T.W.; Sack, P.J.; et al. Trace Element Content of Sedimentary Pyrite as a New Proxy for Deep-Time Ocean—Atmosphere Evolution. *Earth Planet. Sci. Lett.* **2014**, *389*, 209–220. [CrossRef]
18. Hnatyshin, D.; Creaser, R.A.; Meffre, S.; Stern, R.A.; Wilkinson, J.J.; Turner, E.C. Understanding the Microscale Spatial Distribution and Mineralogical Residency of Re in Pyrite: Examples from Carbonate-Hosted Zn-Pb Ores and Implications for Pyrite Re-Os Geochronology. *Chem. Geol.* **2020**, *533*, 119427. [CrossRef]
19. Stein, H.J.; Morgan, J.W.; Scherstén, A. Re-Os Dating of Low-Level Highly Radiogenic (LLHR) Sulfides: The Harnäs Gold Deposit, Southwest Sweden, Records Continental-Scale Tectonic Events. *Econ. Geol.* **2000**, *95*, 1657–1672. [CrossRef]
20. Morelli, R.M.; Creaser, R.A.; Selby, D.; Kelley, K.D.; Leach, D.L.; King, A.R. Re-Os Sulfide Geochronology of the Red Dog Sediment-Hosted Zn-Pb-Ag Deposit, Brooks Range, Alaska. *Econ. Geol.* **2004**, *99*, 1569–1576. [CrossRef]
21. Lawley, C.; Selby, D.; Imber, J. Re-Os Molybdenite, Pyrite and Chalcopyrite Geochronology, Lupa Goldfield, Southwestern Tanzania: Tracing Metallogenic Time Scales at Midcrustal Shear Zones Hosting Orogenic Au Deposits. *Econ. Geol.* **2013**, *108*, 1591–1613. [CrossRef]
22. Hnatyshin, D.; Creaser, R.A.; Wilkinson, J.J.; Gleeson, S.A. Re-Os Dating of Pyrite Confirms an Early Diagenetic Onset and Extended Duration of Mineralization in the Irish Zn-Pb Ore Field. *Geology* **2015**, *43*, 143–146. [CrossRef]
23. Ding, C.; Nie, F.; Bagas, L.; Dai, P.; Jiang, S.; Ding, C.; Liu, C.; Peng, Y.; Zhang, G.; Shao, G. Pyrite Re-Os and Zircon U-Pb Dating of the Tugurige Gold Deposit in the Western Part of the Xing'an-Mongolia Orogenic Belt, China and Its Geological Significance. *Ore Geol. Rev.* **2016**, *72*, 669–681. [CrossRef]

24. Tessalina, S.G.; Herrington, R.J.; Taylor, R.N.; Sundblad, K.; Maslennikov, V.V.; Orgeval, J.J. Lead Isotopic Systematics of Massive Sulphide Deposits in the Urals: Applications for Geodynamic Setting and Metal Sources. *Ore Geol. Rev.* **2016**, *72*, 22–36. [CrossRef]
25. Mathur, R.; Mutti, L.; Barra, F.; Gold, D.; Smith, R.C.; Doden, A.; Detrie, T.; Ruiz, J.; McWilliams, A. Fluid Inclusion and Re-Os Isotopic Evidence for Hot, Cenozoic Mineralization in the Central Pennsylvanian Valley and Ridge Province. *Mineral. Petrol.* **2008**, *93*, 309–324. [CrossRef]
26. Jiang, S.H.; Bagas, L.; Liang, Q.L. Pyrite Re-Os Isotope Systematics at the Zijinshan Deposit of SW Fujian, China: Constraints on the Timing and Source of Cu-Au Mineralization. *Ore Geol. Rev.* **2017**, *80*, 612–622. [CrossRef]
27. Christensen, J.N.; Halliday, A.N.; Leigh, K.E.; Randell, R.N.; Kesler, S.E. Direct Dating of Sulfides by RbSr: A Critical Test Using the Polaris Mississippi Valley-Type ZnPb Deposit. *Geochim. Cosmochim. Acta* **1995**, *59*, 5191–5197. [CrossRef]
28. Petke, T.; Diamond, L.W. Rb-Sr Dating of Sphalerite Based on Fluid Inclusion-Host a Clarification of Why It Works Mineral. *Econ. Geol.* **1996**, *91*, 951–956. [CrossRef]
29. Smith, P.E.; Evensen, N.M.; York, D.; Szatmari, P.; Oliveira, D.C. Single-Crystal Ar-^{39}Ar Dating of Pyrite: No Fool' s Clock. *Geology* **2001**, *29*, 403–406. [CrossRef]
30. Yang, J.H.; Zhou, X.H. Rb-Sr, Sm-Nd and Pb Isotopes Systematics of Pyrite: Implications for the Age and Genesis of Lode Gold Deposits. *Geology* **2002**, *29*, 711–714. [CrossRef]
31. Ivanov, A.V.; Vanin, V.A.; Demonterova, E.I.; Gladkochub, D.P.; Donskaya, T.V.; Gorovoy, V.A. Application of the 'No Fool' s Clock' to Dating the Mukodek Gold Field, Siberia, Russia. *Ore Geol. Rev.* **2015**, *69*, 352–359. [CrossRef]
32. Prokin, V.A.; Buslaev, F.P. Massive Copper-Zinc Sulphide Deposits in the Urals. *Ore Geol. Rev.* **1998**, *14*, 1–69. [CrossRef]
33. Vikentyev, I.V.; Yudovskaya, M.A.; Mokhov, A.V.; Kerzin, A.L.; Tsepin, A.I. Gold and PGE in Massive Sulfide Ore of the Uzelginsk Deposit, Southern Urals, Russia. *Can. Mineral.* **2004**, *42*, 651–665. [CrossRef]
34. Ivanov, S.N.; Prokin, V.A. *Copper Massive Sulfide Deposits of the Urals. Conditions of Formation*; Ural branch of RAS: Ekaterinburg, Russia, 1992.
35. Seravkin, I.B. Correlation between Compositions of Ore and Host Rocks in Volcanogenic Massive Sulfide Deposits of the Southern Urals. *Geol. Ore Depos.* **2013**, *55*, 207–224. [CrossRef]
36. Baranov, E.N.; Schteinberg, A.D.; Karpukhina, V.S. A Genetic Model and Exploration Criteria for Buried Massive Sulphide Deposits of the Verkhneuralsky Area, Southern Urals, USSR. In Proceedings of the 7th IAGOD Symposium, Luleå, Sweden, 18–22 August 1986; pp. 449–460.
37. Seravkin, I.B.; Kosarev, A.M.; Puchkov, V.N. Geodynamic Conditions of Formation of Massive Sulfide Deposits in the Magnitogorsk Megazone, Southern Urals and Prospection Criteria. *Geol. Ore Depos.* **2017**, *59*, 227–243. [CrossRef]
38. Barrie, C.T.; Hannington, M. Introduction: Classification of VMS Deposits Based on Host Rock Composition. In Volcanic-Associated Massive Sulfide Deposits: Processes and Examples in Modern and Ancient Settings. *Rev. Econ. Geol.* **1999**, *8*, 2–10.
39. Franklin, J.M.; Gibson, H.L.; Jonasson, I.R.; Galley, A.G. Volcanogenic Massive Sulfide Deposits. *Econ. Geol. 100th Anniversary Vol.* **2005**, *98*, 523–560.
40. Maslennikov, V. *Lithogenesis and Ore Formation*; Ural Branch RAS: Miass, Russia, 2006.
41. Herrington, R.; Maslennikov, V.; Zaykov, V.; Seravkin, I.; Kosarev, A.; Buschmann, B.; Orgeval, J.J.; Holland, N.; Tesalina, S.; Nimis, P.; et al. 6: Classification of VMS Deposits: Lessons from the South Uralides. *Ore Geol. Rev.* **2005**, *27*, 203–237. [CrossRef]
42. Galley, A.G.; Hannington, M.D.; Jonasson, I.R. Volcanogenic Massive Sulphide Deposits. In *Mineral Deposits of Canada: A Synthesis of Major Deposit-types, District Metallogeny, the Evolution of Geological Provinces and Exploration Methods*; Special Publication No., 5; Goodfellow, W.D., Ed.; Geological Association of Canada, Mineral Deposits Division: Ottawa, Canada, 2007; pp. 141–162.
43. Shanks, W.C.P.; Thurston, R. *Volcanogenic Massive Sulfide Occurrence Model*; Scientific Investigations Report 2010–5070–C; U.S. Geological Survey: Reston, VA, USA, 2012.
44. Ayupova, N.R.; Maslennikov, V.V. Biomineralization in Ferruginous-Siliceous Sediments of Massive Sulfide Deposits of the Urals. *Dokl. Earth Sci.* **2012**, *442*, 193–195. [CrossRef]

45. Maslennikov, V.V.; Ayupova, N.R.; Herrington, R.J.; Danyushevskiy, L.V.; Large, R.R. Ferruginous and Manganiferous Haloes around Massive Sulphide Deposits of the Urals. *Ore Geol. Rev.* **2012**, *47*, 5–41. [CrossRef]
46. Vikentyev, I.V.; Belen'kaya, Y.A.; Ageev, B.I. The Aleksandrinsk Polymetallic Massive Sulfide Deposit (the Urals, Russia). *Geol. Ore Depos.* **2000**, *42*, 221–246.
47. Zaykov, V.V. *Volcanism and Sulfide Hills of Paleooceanic Margins by the Example of Pyrite Zones of the Urals and Siberia*; Nauka: Moscow, Russia, 2006.
48. Hannington, M.D. Volcanogenic Massive Sulfide Deposits. In *Treatise on Geochemistry*, Geochemistry of Mineral, Deposits; Scott, S.D., Ed.; 2nd ed.; Elsevier: Amsterdam, The Netherlands, 2014; Volume 13, pp. 462–486.
49. Maslennikov, V.V.; Maslennikova, S.P.; Large, R.R.; Danyushevsky, L.V.; Herrington, R.J.; Ayupova, N.R.; Zaykov, V.V.; Lein, A.Y.; Tseluyko, A.S.; Melekestseva, I.Y.; et al. Chimneys in Paleozoic Massive Sulfide Mounds of the Urals VMS Deposits: Mineral and Trace Element Comparison with Modern Black, Grey, White and Clear Smokers. *Ore Geol. Rev.* **2017**, *85*, 64–106. [CrossRef]
50. Maslennikov, V.V.; Ayupova, N.R.; Safina, N.P.; Tseluyko, A.S.; Melekestseva, I.Y.; Large, R.R.; Herrington, R.J.; Kotlyarov, V.A.; Blinov, I.A.; Maslennikova, S.P.; et al. Mineralogical Features of Ore Diagenites in the Urals Massive Sulfide Deposits, Russia. *Minerals* **2019**, *9*, 150. [CrossRef]
51. Reiners, P.W.; Carlson, R.W.; Renne, P.; Cooper, K.M.; Granger, D.E.; McLean, N.M.; Schoene, B. *Geochronology and Thermochronology*; Wiley & Sons: Hoboken, NJ, USA, 2017; pp. 291–363.
52. Butler, I.B.; Nesbitt, R.W. Trace Element Distributions in the Chalcopyrite Wall of a Black Smoker Chimney: Insights from Laser Ablation Inductively Coupled Plasma Mass Spectrometry (LA-ICP-MS). *Earth Planet. Sci. Lett.* **1999**, *167*, 335–345. [CrossRef]
53. Melekestseva, I.Y.; Tret'yakov, G.A.; Nimis, P.; Yuminov, A.M.; Maslennikov, V.V.; Maslennikova, S.P.; Kotlyarov, V.A.; Beltenev, V.E.; Danyushevsky, L.V.; Large, R. Barite-Rich Massive Sulfides from the Semenov-1 Hydrothermal Field (Mid-Atlantic Ridge, 13°30.87′ N): Evidence for Phase Separation and Magmatic Input. *Mar. Geol.* **2014**, *349*, 37–54. [CrossRef]
54. Baranov, E.N.; Vertepov, G.I. Concentration of Uranium in Sulphides as an Indicator of Possible Uranium Deposit. *At. Energy* **1966**, *20*, 170–171. [CrossRef]
55. Liu, G.Q.; Zhao, K.D.; Jiang, S.Y.; Chen, W. In-Situ Sulfur Isotope and Trace Element Analysis of Pyrite from the Xiwang Uranium Ore Deposit in South China: Implication for Ore Genesis. *J. Geochem. Explor.* **2018**, *195*, 49–65. [CrossRef]
56. Wang, L.; Wang, X.; Ye, J.; Ma, Z.; Yang, W.; Xiao, J. Separation of Uranium and Thorium for ^{230}Th-U Dating of Submarine Hydrothermal Sulfides. *J. Vis. Exp.* **2019**, *2019*, 1–6. [CrossRef]
57. Eglizaud, B.N.; Miserque, F.; Simoni, E.; Schlegel, M.; Descostes, M. Uranium (VI) Interaction with Pyrite (FeS_2). *Radiochim. Acta* **2006**, *94*, 651–656. [CrossRef]
58. Descostes, M.; Schlegel, M.L.; Eglizaud, N.; Descamps, F.; Miserque, F.; Simoni, E. Uptake of Uranium and Trace Elements in Pyrite (FeS_2) Suspensions. *Geochim. Cosmochim. Acta* **2010**, *74*, 1551–1562. [CrossRef]
59. Yarosh, P.Y. *Diagenez i Metamorfizm Kolchedannykh Rud Na Urale (Diagenesis and Metamorphism of Sulfide Ores at the Urals)*; Nauka: Moscow, Russia, 1973.
60. Kailachakov, P.E.; Doynikova, O.A.; Belousov, P.E.; Vikentyev, I.V. Unique Rhenium Deposit in the Carboniferous Coal-Bearing Sands of the Russian Plate: Communication 2. Ore Mineralogy. *Lithol. Miner. Resour.* **2020**, *55*, 337–370. [CrossRef]
61. Garuti, G.; Zaccarini, F. Minerals of Au, Ag and U in Volcanic-Rock-Associated Massive Sulfide Deposits of the Northern Apennine Ophiolite, Italy. *Can. Mineral.* **2005**, *43*, 935–950. [CrossRef]
62. Murzin, V.V.; Varlamov, D.A.; Vikentyev, I.V. Copper–Cobalt Mineralization of the Pyshmin-Klyuchevskoy Deposit, Middle Urals: Mineral Composition of Ores and Metasomatites, Staged Formation and P–T Conditions of Formation. *Litosfera* **2011**, *6*, 103–122.
63. Moloshag, V.P. Radioactive Mineralization of Supergene Ores of Sulfide Deposits of the Urals by the Example of the Tan'er Deposit. *Ezhegodnik* **2015**, *162*, 169–171.
64. Ayupova, N.R.; Melekestseva, I.Y.; Maslennikov, V.V.; Tseluyko, A.S.; Blinov, I.A.; Beltenev, V.E. Uranium Accumulation in Modern and Ancient Fe-Oxide Sediments: Examples from the Ashadze-2 Hydrothermal Sulfide Field (Mid-Atlantic Ridge) and Yubileynoe Massive Sulfide Deposit (South Urals, Russia). *Sediment. Geol.* **2018**, *367*, 164–174. [CrossRef]

65. Farley, K.A.; Wolf, R.A.; Silver, L.T. The Effects of Long Alpha-Stopping Distances on (U-Th)/He Ages. *Geochim. Cosmochim. Acta* **1996**, *60*, 4223–4229. [CrossRef]
66. Ziegler, J.F.; Ziegler, M.D.; Biersack, J.P. SRIM—The Stopping and Range of Ions in Matter. *Nucl. Inst. Methods Phys. Res. B* **2010**, *268*, 1818–1823. [CrossRef]
67. Stuart, F.M.; Burnard, P.G.; Taylor, R.P.; Turner, G. Resolving Mantle and Crustal Contributions to Ancient Hydrothermal Fluids: HeAr Isotopes in Fluid Inclusions from Dae Hwa WMo Mineralisation, South Korea. *Geochim. Cosmochim. Acta* **1995**, *59*, 4663–4673. [CrossRef]
68. Burnard, P.G.; Hu, R.; Turner, G.; Bi, X.W. Mantle, Crustal and Atmospheric Noble Gases in Ailaoshan Gold Deposits, Yunnan Province, China. *Geochim. Cosmochim. Acta* **1999**, *63*, 1595–1604. [CrossRef]
69. Burnard, P.G.; Polya, D.A. Importance of Mantle Derived Fluids during Granite Associated Hydrothermal Circulation: He and Ar Isotopes of Ore Minerals from Panasqueira. *Geochim. Cosmochim. Acta* **2004**, *68*, 1607–1615. [CrossRef]
70. Kendrick, M.A.; Burgess, R.; Pattrick, R.A.D.; Turner, G. Fluid Inclusion Noble Gas and Halogen Evidence on the Origin of Cu-Porphyry Mineralising Fluids. *Geochim. Cosmochim. Acta* **2001**, *65*, 2651–2668. [CrossRef]
71. Stuart, F.M.; Turner, G.; Duckworth, R.C.; Fallick, A.E. Helium Isotopes as Tracers of Trapped Hydrothermal Fluids in Ocean-Floor Sulfides. *Geology* **1994**, *22*, 823–826. [CrossRef]
72. Jean-Baptiste, P.; Fouquet, Y. Abundance and Isotopic Composition of Helium in Hydrothermal Sulfides from the East Pacific Rise at 13°N. *Geochim. Cosmochim. Acta* **1996**, *60*, 87–93. [CrossRef]
73. Bortnikov, N.S.; Vikentyev, I.V.; Stavrova, O.O.; Ikorskii, S.V.; Kamenskii, I.L.; Bogdanov, Y.A.; Avedisyan, A.A. Helium Isotopic Composition and Hydrocarbons in Fluid Inclusions from Serpentinites and Sulfides of the Logachev and Rainbow Hydrothermal Fields, Mid-Atlantic Ridge. *Dokl. Earth Sci.* **2000**, *375*, 1387–1390.
74. Bortnikov, N.; Ikorskii, S.; Kamenskii, I.; Avetisyan, A.; Simonov, V.; Bogdanov, Y.; Lein, A.; Sagalevich, A.; Vikentyev, I.; Stavrova, O. Modem Sulfide Ores at Mid-Atlantic Ridge and Pacific Back-Arc Basins: Fluid Inclusion, Hydrocarbon and He, Ar and S Isotope Studies. In *Mineral Exploration and Sustainable Development*; Eliopoulous, D.G., Ed.; Millpress: Rotterdam, The Netherlands, 2003; pp. 115–118.
75. Luders, V.; Niedermann, S. Helium isotope composition of fluid inclusions hosted in massive sulfides from modern submarine hydrothermal systems. *Sci. Commun.* **2010**, *105*, 443–449. [CrossRef]
76. Bierens de Haan, S. A Review of the Rate of Pyrite Oxidation in Aqueous Systems at Low Temperature. *Earth Sci. Rev.* **1991**, *31*, 1–10. [CrossRef]
77. Stein, H.J.; Sundblad, K.; Markey, R.J.; Morgan, J.W.; Motuza, G. Re-Os Ages for Archean Molybdenite and Pyrite, Kuittila-Kivisuo, Finland and Proterozoic Molybdenite, Kabeliai, Lithuania: Testing the Chronometer in a Metamorphic and Metasomatic Setting. *Miner. Depos.* **1998**, *33*, 329–345. [CrossRef]
78. van Acken, D.; Su, W.; Gao, J.; Creaser, R.A. Preservation of Re-Os Isotope Signatures in Pyrite throughout Low-T, High-P Eclogite Facies Metamorphism. *Terra Nov.* **2014**, *26*, 402–407. [CrossRef]
79. Vernon, R.; Holdsworth, R.E.; Selby, D.; Dempsey, E.; Finlay, A.J.; Fallick, A.E. Structural Characteristics and Re-Os Dating of Quartz-Pyrite Veins in the Lewisian Gneiss Complex, NW Scotland: Evidence of an Early Paleoproterozoic Hydrothermal Regime during Terrane Amalgamation. *Precambrian Res.* **2014**, *246*, 256–267. [CrossRef]
80. Smirnov, V.I. *Copper Massive Sulfide Deposits of the Urals. Geology*; Ural Branch USSR AS: Sverdlovsk, Russia, 1988.
81. Vikentyev, I.V.; Karpukhina, V.S. Uzelginsk Zn-Cu-Ag VMS Deposit, South Urals: Genetic Aspect. In *Applied Mineralogy*; Rammlmair, D., Ed.; Balkema: Rotterdam, The Netherlands, 2000; pp. 455–458.
82. Bortnikov, N.S.; Vikentyev, I.V. Endogenous Metallogeny of the Urals. In *Mineral Deposit Research for a High-Tech World*; Jonsson, E., Ed.; Sverige AB: Uppsala, Sweden, 2013; pp. 1508–1511.
83. Maslov, V.A.; Artyushkova, O.V. *Stratigraphy of Paleozoic Formations of Uchaly District of Bashkiria*; Institute of Geology Ufa Scientific Center RAS: Ufa, Russia, 2000.
84. Kontar', E.S. *The Geological-Industrial Types of the Cu, Zn, Pb Deposits in the Urals (Geological Conditions of Setting, History of the Formation, the Prospects)*; Uralian Mining-Geol. Uni. Publ: Ekaterinburg, Russia, 2013.
85. Puchkov, V.N. General Features Relating to the Occurrence of Mineral Deposits in the Urals: What, Where, When and Why. *Ore Geol. Rev.* **2017**, *85*, 4–29. [CrossRef]
86. Becker, T.R.; Gradstein, F.M.; Hammer, Ø. The Devonian Period. In *The Geologic Time Scale*; Gradstein, F.M., Ogg, J.G., Schmitz, M., Ogg, G., Eds.; Elsevier: Amsterdam, The Netherlands, 2012; Volume 1–2, pp. 559–601. [CrossRef]

87. Vikentyev, I.; Chugaev, A.; Karpukhina, V.S.; Nosik, L.; Rimskaya-Korsakova, M. Origin of Uzelginsk Zn-Cu-Ag VHMS Deposit, Southern Urals. In *12th IAGOD Symp. "Understanding the Genesis of Ore Deposits to Meet the Demands of the 21st Century"*; Elsevier Science B.V.: Amsterdam, The Netherlands, 2006; pp. 1233–1236.
88. Amplieva, A.A.; Vikent'Yev, I.V.; Karpukhina, V.S.; Bortnikov, N.S. The Role of Magmatogene Fluid in the Formation of the Talgan Copper–Zinc–Pyritic Deposit, Southern Urals. *Dokl. Earth Sci.* **2008**, *423*, 1427–1430. [CrossRef]
89. Vikentev, I.V.; Borisova, A.Y.; Karpukhina, V.S.; Naumov, V.B.; Ryabchikov, I.D. Direct Data on the Ore Potential of Acid Magmas of the Uzel'ginskoe Ore Field (Southern Urals, Russia). *Dokl. Earth Sci.* **2012**, *443*(1), 401–405. [CrossRef]
90. Pirozhok, P.I.; Chadchenko, A.V. On the Productivity of the Copper-Zinc-Pyrite XIX Parts'ezda Deposit, South Urals: To the 60th Anniversary of the Discovery. In *Metallogeny of Ancient and Modern Oceans*; Institute of Mining of the Ural Branch of the Russian Academy of Sciences: Miass, Russia, 2012; pp. 303–307.
91. Zavaritsky, A.N. Metamorphism and Metasomatism in the Urals Pyrite Deposits. In *Massive Sulphide Deposits of the Urals*; Acad. Sci. Publ.: Moscow, Russia, 1950; pp. 7–18.
92. Shadlun, T.N. Features of the Mineralogical Composition, Structures and Textures of Ores of Somemassive Sulphide Deposits of the Urals. In *Massive Sulphide Deposits of the Urals*; USSR AS: Moscow, Russia, 1950; pp. 117–147.
93. Vikentyev, I.V.; Belogub, E.V.; Novoselov, K.A.; Moloshag, V.P. Metamorphism of Volcanogenic Massive Sulphide Deposits in the Urals. Ore Geology. *Ore Geol. Rev.* **2017**, *85*, 30–63. [CrossRef]
94. Tessalina, S.G.; Jourdan, F.; Belogub, E.V. Significance of Late Devonian—Lower Carboniferous Ages of Hydrothermal Sulphides and Sericites from the Urals Volcanic-Hosted Massive Sulphide Deposits. *Ore Geol. Rev.* **2017**, *85*, 131–139. [CrossRef]
95. Gannoun, A.; Tessalina, S.; Bourdon, B.; Orgeval, J.J.; Birck, J.L.; Allègre, C.J. Re-Os Isotopic Constraints on the Genesis and Evolution of the Dergamish and Ivanovka Cu (Co, Au) Massive Sulphide Deposits, South Urals, Russia. *Chem. Geol.* **2003**, *196*, 193–207. [CrossRef]
96. Tessalina, S.G.; Bourdon, B.; Maslennikov, V.V.; Orgeval, J.J.; Birck, J.L.; Gannoun, A.; Capmas, F.; Allègre, C.J. Osmium Isotope Distribution within the Palaeozoic Alexandrinka Seafloor Hydrothermal System in the Southern Urals, Russia. *Ore Geol. Rev.* **2008**, *33*, 70–80. [CrossRef]
97. Chernyshev, I.V.; Vikent'ev, I.V.; Chugaev, A.V.; Shatagin, K.N.; Moloshag, V.P. Sources of Material for Massive Sulfide Deposits in the Urals: Evidence from the High-Precision MC-ICP-MS Isotope Analysis of Pb in Galena. *Dokl. Earth Sci.* **2008**, *418*, 178–183. [CrossRef]
98. Vikent'eva, O.; Prokofiev, V.; Borovikov, A.; Kryazhev, S.; Groznova, E.; Pritchin, M.; Vikentyev, I.; Bortnikov, N. Contrasting Fluids in the Svetlinsk Gold-Telluride Hydrothermal System, South Urals. *Minerals* **2020**, *10*, 37. [CrossRef]
99. Petrov, G.V.; Kazakova, N.M. Geological Structure of the Uzelga Copper-Zinc-Pyritic Deposit. In *Geology and Genesis of ore deposits in the Southern Urals*; Bashkirian branch USSR AS: Ufa, Russia, 1978; pp. 54–63.
100. Vikentyev, I.V. Invisible and Microscopic Gold in Pyrite: New Data for Volcanogenic Massive Sulphide Ores of the Urals. In *Mineral Resources in a Sustainable World*; Andre-Mayer, A.S., Cathelineau, M., Muchez, P., Pirard, E., Sindern, S., Eds.; Université de Lorraine: Nancy, France, 2015; pp. 2113–2116.
101. Vikentyev, I. Selenium, Tellurium and Precious Metal Mineralogy in Uchalinsk Copper-Zinc-Pyritic District, the Urals. In Proceedings of the 3rd International Conference on Competitive Materials and Technology Processes (IC-CMTP3), Miskolc-Lillafüred, Hungary, 6–10 October 2014; Volume 123, pp. 1–6. [CrossRef]
102. Yakubovich, O.V.; Shukolyukov, Y.A.; Kotov, A.B.; Brauns, M.; Samsonov, A.V.; Komarov, A.N.; Yakovleva, S.Z.; Sal'nikova, E.B.; Gorokhovskii, B.M. U-Th-He Dating of Native Gold: First Results, Problems and Outlooks. *Petrology* **2014**, *22*, 429–437. [CrossRef]
103. Dolesal, A.; Povondra, P.; Shultsek, Z. *Methods of Decompostion of Rocks*; MIR: Moscow, Russia, 1968.
104. Vermeesch, P. Three New Ways to Calculate Average (U-Th)/He Ages. *Chem. Geol.* **2008**, *249*, 339–347. [CrossRef]
105. Meesters, A.G.C.A.; Dunai, T.J. A Noniterative Solution of the (U- -Th)//He Age Equation. *Geochem. Geophys. Geosyst.* **2005**, *6*, 1–3. [CrossRef]
106. Vermeesch, P. HelioPlot and the Treatment of Overdispersed (U–Th–Sm)/He Data. *Chem. Geol.* **2010**, *271*, 108–111. [CrossRef]

107. Foeken, J.P.T.; Stuart, F.M.; Dobson, K.J.; Persano, C.; Vilbert, D. A Diode Laser System for Heating Minerals for (U-Th)/He Chronometry. *Geochem. Geophys. Geosyst.* **2006**, *7*. [CrossRef]
108. Orlov, A.K. Stage-by-Stage Oxidation of Sulfides during Oxidative Roasting of Polymineral Sulfide Concentrates. *Zap. Gorn. Inst.* **2006**, *169*, 163–166.
109. Chepushtanova, T.A. *Physico-Chemical Properties and Technological Basis for the Production of Pyrrhotite from Pyrite*; Satbayev University: Almaty, Kazakhstan, 2009; p. 124.
110. Boyanov, B.; Peltekov, A.; Petkova, V. Thermal Behavior of Zinc Sulfide Concentrates with Different Iron Content at Oxidative Roasting. *Thermochim. Acta* **2014**, *586*, 9–16. [CrossRef]
111. Ludwig, K.R. Isoplot 3.00: A Geochronological Toolkit for Microsoft Excel. *Berkeley Geochronol. Cent. Spec. Publ.* **2003**, *4*, 70.
112. Fourre, E.; Jean-Baptiste, P.; Charlou, J.L.; Donval, J.P.; Ishibashi, J.I. Helium Isotopic Composition of Hydrothermal Fluids from the Manus Back-Arc Basin, Papua New Guinea. *Geochem. J.* **2006**, *40*, 245–252. [CrossRef]
113. Zeng, Z.; Niedermann, S.; Chen, S.; Wang, X.; Li, Z. Noble Gases in Sulfide Deposits of Modern Deep-Sea Hydrothermal Systems: Implications for Heat Fluxes and Hydrothermal Fluid Processes. *Chem. Geol.* **2015**, *409*, 1–11. [CrossRef]
114. Stuart, F.M.; Duckworth, R.; Turner, G.; Schofield, P.F. Helium and Sulfur Isotopes of Sulfide Minerals from Middle Valley. *Proc. Ocean Drill. Progr. Sci. Results* **1994**, *139*, 387–392.
115. Vikentyev, I. *Formation Conditions and Metamorphism of VMS Ores*; Nauch mir: Moscow, Russia, 2004.
116. Karpukhina, V.S.; Naumov, V.B.; Vikent'ev, I.V. Genesis of Massive Sulfide Deposits in the Verkhneural'sk Ore District, the South Urals, Russia: Evidence for Magmatic Contribution of Metals and Fluids. *Geol. Ore Depos.* **2013**, *55*, 125–143. [CrossRef]
117. Vikentyev, I.; Simonov, V.A.; Borisova, A.Y.; Karpukhina, V.S.; Naumov, V.B. Volcanic-Hosted Massive Sulphide Deposits of the Urals, Russia: Evidence for a Magmatic Contribution of Metals and Fluid. In *Mineral Deposit Research for a High-Tech World*; Jonsson, E., Ed.; Sverige AB: Uppsala, Sweden, 2013; pp. 1526–1529.
118. Vikentyev, I. Composition of Native Gold in Massive Sulfide Ores of the Urals. *Dokl. Earth Sci.* **2003**, *393*, 1284–1288.
119. Robinson, L.F.; Belshaw, N.S.; Henderson, G.M. U and Th Concentrations and Isotope Ratios in Modern Carbonates and Waters from the Bahamas. *Geochim. Cosmochim. Acta* **2004**, *68*, 1777–1789. [CrossRef]
120. Yarosh, P.Y.; Buslaev, F.P. *Ore Textures and History of Formation of Ore Aggregates of Uzelginsk Deposits*; Nauka: Sverdlovsk, Russia, 1985.
121. Vermeesch, P.; Seward, D.; Latkoczy, C.; Wipf, M.; Günther, D.; Baur, H. α-Emitting Mineral Inclusions in Apatite, Their Effect on (U-Th)/He Ages and How to Reduce It. *Geochim. Cosmochim. Acta* **2007**, *71*, 1737–1746. [CrossRef]